EPJ manuscript No.
(will be inserted by the editor)

Quark–gluon vertex in general kinematics

Ayşe Kızılersü[1], Derek B. Leinweber[1], Jon-Ivar Skullerud[2], and Anthony G. Williams[1]

[1] Centre for the Subatomic Structure of Matter, Adelaide University, Adelaide, SA 5005, Australia
[2] School of Mathematics, Trinity College, Dublin 2, Ireland

the date of receipt and acceptance should be inserted later

Abstract. We compute the quark-gluon vertex in quenched lattice QCD, in the Landau gauge using an off-shell mean-field $\mathcal{O}(a)$-improved fermion action. The Dirac-vector part of the vertex is computed for arbitrary kinematics. We find a substantial infrared enhancement of the interaction strength regardless of kinematics.

1 Introduction

In recent years, substantial progress has been made in our understanding of the nonperturbative correlation functions (propagators and vertices) of the fundamental fields of QCD and their relation to the phenomena of colour confinement and dynamical chiral symmetry breaking. It has emerged that at least in Landau gauge, a detailed knowledge of the structure of the quark–gluon vertex is essential for an understanding of the dynamics of quark confinement and chiral symmetry breaking as encoded in the quark Dyson–Schwinger equation (DSE), relating the quark propagator $S(p)$ to the gluon propagator and the quark–gluon vertex $\Gamma_\mu(p,q)$, where p and q are quark and gluon momenta respectively:

$$\begin{aligned} S^{-1}(p) &= i\not{p} + m \\ &\quad + \frac{4g^2}{3}\int\frac{d^4q}{(2\pi)^4}\gamma_\mu S(p-q)D_{\mu\nu}(q)\Gamma_\nu(p-q,q) \,. \end{aligned} \tag{1}$$

Here, $D_{\mu\nu}(q) = P_{\mu\nu}(q)D(q^2)$ is the gluon propagator, with $P_{\mu\nu}(q)$ the transverse projection operator.

The overall shape of the gluon propagator is now quite well known, both from lattice QCD [1–3] and from studies of the coupled ghost–gluon Dyson–Schwinger equations. It is now clear that if this is fed into the quark DSE together with a bare or QED-like vertex, the resulting quark propagator will not exhibit a sufficient degree of chiral symmetry breaking [4–7].

The quark–gluon vertex is related to the ghost sector through the Slavnov–Taylor identity (STI),

$$\begin{aligned} q^\mu\Gamma_\mu(p,q) = G(q^2)\Big[&(1-B(q,p+q))S^{-1}(p) \\ &- S^{-1}(p+q)(1-B(q,p+q))\Big] \,, \end{aligned} \tag{2}$$

where $G(q^2)$ is the ghost renormalisation function and $B^a(q,k)$ is the ghost–quark scattering kernel. In particular, if the ghost propagator is infrared enhanced, as both lattice [8,3] and DSE studies [9] indicate, the vertex will also be so. This provides for a consistent picture of confinement and chiral symmetry breaking at the level of the Green's functions of Landau-gauge QCD, where the same infrared enhancement that is responsible for confinement of gluons, provides the necessary interaction strength to give rise to dynamical chiral symmetry breaking in the quark sector.

Confinement of quarks is still not fully understood in this picture, however. If the effective interaction between a quark and an antiquark by way of exchange of a nonperturbative gluon is to give rise to a linearly confining potential, the quark–gluon vertex must contain an infrared enhancement over and above that contained in the ghost self-energy. A recent DSE calculation [10] indicates that this may indeed be the case, with te running coupling α_{qg} defined from this vertex diverging quadratically in the infrared.

In two previous papers [11,12] the quark–gluon vertex was computed on the lattice in two specific kinematics. Those results indicate a highly nontrvial infrared tensor structure, a result that has been qualitatively supported by semiperturbative DSE-based calculations [7,13]. However, these kinematics may not dominate the DSE (1). It is therefore necessary to compute the vertex in arbitrary kinematics, as far as possible. This is the focus of the present paper, although at this point we will be restricting ourselves to the dominant, vector part of the vertex. Preliminary results were reported in [14].

The structure of this article is as follows: In sec. 2 we briefly recap the formalism used in these studies. The main results are contained in sec. 3, while in sec. 4 we discuss the implications and possible future directions. Some tree-level lattice formulae are contained in the Appendix.

2 Formalism

We denote the outgoing quark momentum p and the outgoing gluon momentum q. The incoming quark momentum is $k = p + q$. In the continuum, the quark–gluon vertex can be decomposed into four components L_i contributing to the Slavnov–Taylor identity and eight purely transverse components T_i:

$$\begin{aligned}\Gamma_\mu(p,q) = &\sum_{i=1}^{4} \lambda_i(p^2,q^2,k^2) L_{i,\mu}(p,q) \\ &+ \sum_{i=1}^{8} \tau_i(p^2,q^2,k^2) T_{i,\mu}(p,q)\,.\end{aligned} \tag{3}$$

The components L_i and T_i are given in Ref.[11]:

$$\begin{aligned}
L_{1,\mu} &= \gamma_\mu & L_{2,\mu} &= -\not{P}P_\mu \\
L_{3,\mu} &= -iP_\mu & L_{4,\mu} &= -i\sigma_{\mu\nu}P_\nu \\
T_{1,\mu} &= -i\ell_\mu & T_{2,\mu} &= -\not{P}\ell_\mu
\end{aligned} \tag{4}$$

$$\begin{aligned}
T_{3,\mu} &= \not{q}q_\mu - q^2\gamma_\mu \\
T_{4,\mu} &= -i\left[q^2\sigma_{\mu\nu}P_\nu + 2q_\mu\sigma_{\nu\lambda}p_\nu k_\lambda\right] \\
T_{5,\mu} &= -i\sigma_{\mu\nu}q_\nu \qquad T_{6,\mu} = (qP)\gamma_\mu - \not{q}P_\mu \\
T_{7,\mu} &= -\frac{i}{2}(qP)\sigma_{\mu\nu}P_\nu - iP_\mu\sigma_{\nu\lambda}p_\nu k_\lambda \\
T_{8,\mu} &= -\gamma_\mu\sigma_{\nu\lambda}p_\nu k_\lambda - \not{p}k_\mu + \not{k}p_\mu
\end{aligned} \tag{5}$$

where $P_\mu \equiv p_\mu + k_\mu$, $\ell_\mu \equiv (pq)k_\mu - (kq)p_\mu$. In Landau gauge, for $q \neq 0$, we are only able to compute the transverse projection of the vertex, $\Gamma^P_\mu(p,q) \equiv P_{\mu\nu}(q)\Gamma_\nu(p,q)$, where $P_{\mu\nu}(q) \equiv \delta_{\mu\nu} - q_\mu q_\nu/q^2$ is the transverse projector. Since the vertex will always be coupled to a gluon propagator which contains the same projector, this is also the only combination that appears in any applications. The four functions $L_{i,\mu}$ are projected onto the transverse $T_{i,\mu}$, giving rise to modified form factors

$$\begin{aligned}
\lambda'_1 &= \lambda_1 - q^2\tau_3\,; & \lambda'_2 &= \lambda_2 - \frac{q^2}{2}\tau_2\,; \\
\lambda'_3 &= \lambda_3 - \frac{q^2}{2}\tau_1\,; & \lambda'_4 &= \lambda_4 + q^2\tau_4\,.
\end{aligned} \tag{6}$$

The lattice tensor structure is more complex, and (3) is only recovered in the continuum. The form factors also receive large contributions from lattice artefacts at tree level, so tree-level correction is required, as described in the Appendix.

3 Results

We have analysed 495 configurations on a $16^3 \times 48$ lattice at $\beta = 6.0$, using a mean-field improved SW action with a quark mass $m \approx 115$ MeV. This is part of the UKQCD data set described in [15]; further details can also be found in [11].

The general lattice tensor structure, even for the Dirac-vector part of the vertex alone, is quite complicated, as the tree-level expression in eq. (14) of the Appendix gives an indication of. This makes a determination of the full tensor structure of the vertex intractable with this lattice action. However, in the special case where both the quark and gluon momentum vectors are chosen to be 'perpendicular' to the vertex, i.e. if we compute $\Gamma_\mu(p,q)$ with $p_\mu = q_\mu = 0$, this structure simplifies considerably. There is no loss of generality provided rotational symmetry is restored in the continuum. We will here only study the leading, vector part of the vertex, as this is expected to have the cleanest signal, and tree-level lattice artefacts can be corrected multiplicatively. In continuum notation, we compute

$$\begin{aligned}
\frac{1}{4}\,\mathrm{tr}\,\gamma_\mu\Gamma^P_\mu(p,q) &= \Big(1 - \frac{q_\mu^2}{q^2}\Big)\lambda'_1 \\
&\quad + \frac{2}{q^2}\Big[(pq)k_\mu - (kq)p_\mu\Big](p_\mu + k_\mu)\lambda'_2 \qquad (7) \\
&\quad - [k^2 - p^2 - (k_\mu^2 - p_\mu^2)]\tau_6 \\
&= \lambda'_1 - (k^2 - p^2)\tau_6 \equiv \lambda''\,. \qquad (8)
\end{aligned}$$

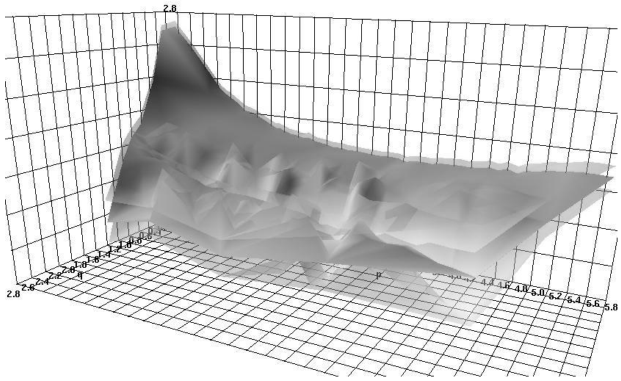

Fig. 1. The unrenormalised form factor λ'_1 in the quark-symmetric kinematics $p^2 = k^2$, as a function of quark momentum p (long axis) and gluon momentum q (short axis). The opaque surfaces denotes the statistical uncertainties.

Of particular interest is the quark-symmetric limit, where the two quark momenta are equal in magnitude, $p^2 = k^2$. In this case, τ_6 is also eliminated, i.e. $\lambda''_1(p^2,q^2,p^2) = \lambda'_1(p^2,q^2,p^2)$. Note that both the soft gluon ("asymmetric") and the quark reflection ("symmetric") kinematics discussed previously in [11,12] are specific instances of this more general case. In fig. 1 we show λ'_1 as a function of the two remaining independent momentum invariants. The data become quite noisy as q in particular is increased, and also exhibit some 'spikes' and 'troughs' which at present we assume to be numerical noise and lattice artefacts. There appears to be some difference in the behaviour as a function of gluon momentum q and quark momentum p, but in view of the noise this cannot be further quantified.

By interpolating the points in fig. 1, we may reach the totally symmetric point where $p^2 = k^2 = q^2$. This kinematics has a history of being used to define a momentum subtraction (MOM) scheme [16]. We show our results in

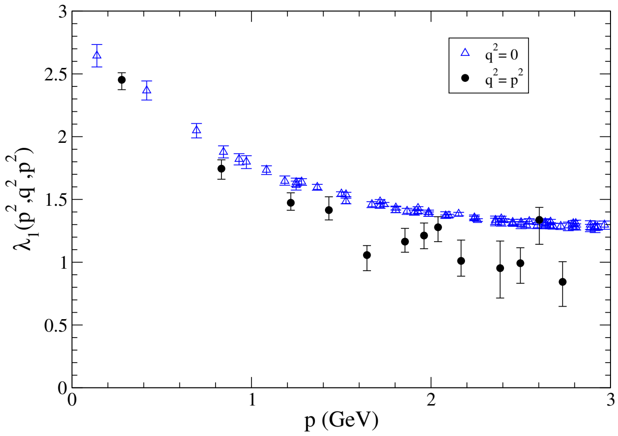

Fig. 2. The unrenormalised form factor λ_1' at the totally symmetric kinematics $p^2 = k^2 = q^2$, as a function of the momentum p. Also shown is the same form factor in the soft gluon kinematics $q^2 = 0$.

fig. 2, together with the data from the soft gluon point presented in [11,12]. Again we find a strong infrared enhancement, comparable to that of the two other kinematics. The qualitative behaviour of λ_1' as a function of p^2 is similar in all three cases, with a tendency to drop more rapidly as q^2 increases, as one would expect if the vertex is infrared enhanced in all momentum variables. It does not appear possible to describe the three momentum directions with a single common variable, i.e. $\lambda_1'(p^2, q^2, p^2) = \bar{\lambda}_1(t^2(p^2, q^2))$. Note that all three data sets should approach the same limit as $p^2 \to 0$.

Finally, figs. 3 and 4 show λ_1'' in general kinematics, for four different fixed values of q, as a function of the two quark momenta p and k. We expect all form factors to be symmetric in p^2 and k^2 (τ_6 on its own is antisymmetric, but is multiplied by $p^2 - k^2$), and this is also what the figures show, within errors. The broadening of the data surface as q grows is simply a reflection of the increase in available phase space.

The same qualitiative features as were found in the more specific kinematics, are reproduced here. At low q, we see a clear infrared enhancement, which disappears as q grows, reflecting the fact that at high momentum scales, only the logarithmic behaviour (which is too weak to be seen in these data) remains. At the same time, the level of the surface sinks, which reflects the infrared enhancement of λ_1'' also as a function of gluon momentum.

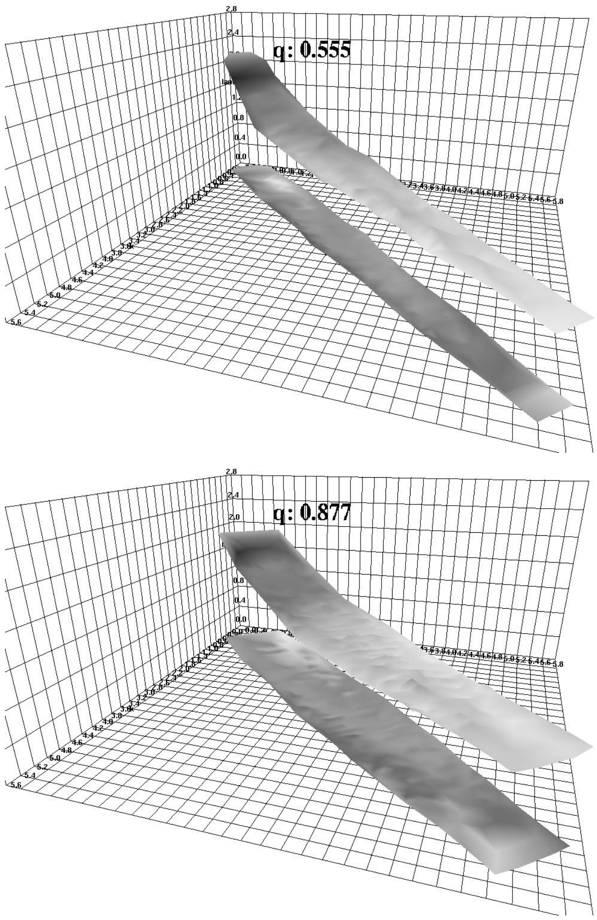

Fig. 3. The unrenormalised form factor λ_1'' for gluon momentum $q = 0.555$ GeV (top) and $q = 0.873$ GeV (bottom), as a function of quark momenta p and k. The lower surfaces denote the statistical uncertainties.

4 Discussion and outlook

We have determined the leading component of the quark–gluon vertex as a function of all three momentum invariants p^2, k^2, q^2. We find an infrared enhancement in all momentum directions, although the quality of the current data does not make a further quantification of this feasible.

These results have been obtained on a rather small lattice, and with a discretisation that gives rise to quite large tree-level lattice artefacts which must be corrected for. We therefore expect systematic errors to be quite large. To obtain more reliable results, and to extend this study to the full vertex structure at all kinematics, it would be desirable to employ an action which is known to have smaller and more tractable tree-level artefacts. The Asqtad action has been employed successfully in computing the quark propagator [17], and unlike the SW action, only λ_1 and possibly λ_2 are non-zero at tree level, so no tree-level correction will be needed for the remaining form factors. This action is also computationally relatively cheap, making large lattice volumes feasible. Another possibility is using overlap fermions, which have the advantage of retaining an exact chiral symmetry, which also protects all the odd Dirac components of the vertex at tree level.

This work has been supported by the Australian Research Council and the Irish Research Council for Science, Engineering and Technology. JIS is grateful for the hospitality of the Centre for the Subatomic Structure of Matter, where part of this work was carried out. We thank Patrick Bowman, Rein-

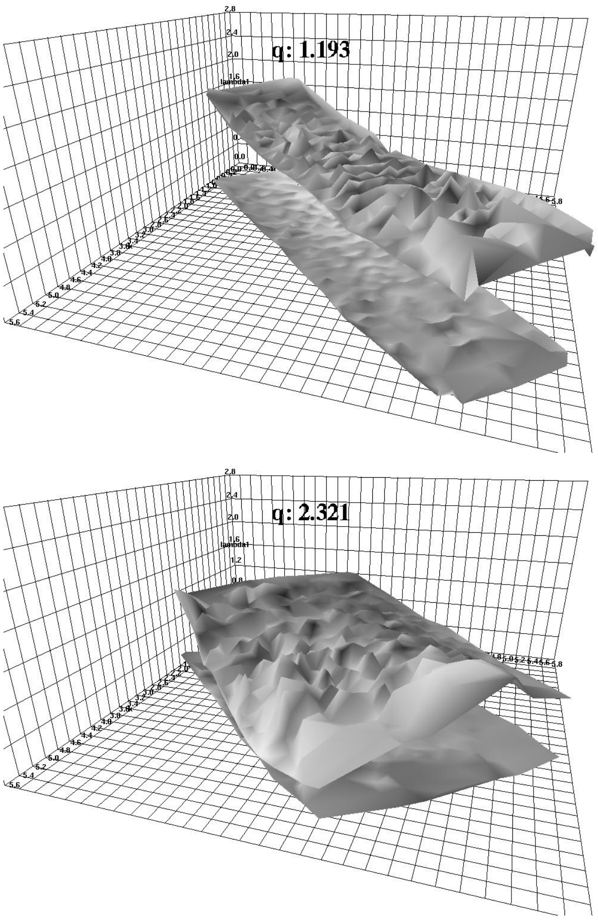

Fig. 4. As fig. 3, but for gluon momentum $q = 1.193$ GeV and 2.321 GeV.

hard Alkofer, Christian Fischer and Craig Roberts for stimulating discussions.

Appendix

We use the same notation as in [12], defining the lattice momentum variables

$$K_\mu(p) \equiv \frac{1}{a}\sin(p_\mu a)\,; \tag{9}$$

$$Q_\mu(p) \equiv \frac{2}{a}\sin(p_\mu a/2)\,; \tag{10}$$

$$C_\mu(p) \equiv \cos(p_\mu a)\,. \tag{11}$$

The tree-level vertex can be written

$$\begin{aligned}\Gamma^{(0)}_{I,\mu}(p,q) &= c_m\Big[i \not{K}(p)A_V(p) + B_V(p)\Big]\times \\ &\times\Big\{\gamma_\mu C_\mu(s) - iK_\mu(s) - i\frac{c_{\rm sw}}{2}C_\mu(q/2)\sum_\nu \sigma_{\mu\nu}K_\nu(q)\Big\}\times \\ &\times\Big[i \not{K}(k)A_V(k) + B_V(k)\Big]/D_I(p)D_I(k)\,,\end{aligned} \tag{12}$$

where $k = p + q; s = P/2 = (p + k)/2; c_m = 1 + b_q ma$; and A_V, B_V and D_I are defined in [12]. The transverse projection is given by

$$\Gamma^{P(0)}_{I,\mu}(p,q) = \sum_\nu\left(\delta_{\mu\nu} - \frac{Q_\mu(q)Q_\nu(q)}{Q^2(q)}\right)\Gamma^{(0)}_{I,\nu}(p,q) \tag{13}$$

Concentrating on the vector part of the vertex, we find that

$$\begin{aligned}&\frac{D_I(p)D_I(k)}{4c_m}\,\mathrm{tr}\Big(\gamma_\mu\Gamma^{P(0)}_{I,\mu}(p,q)\Big) \\ &= C_\mu(s)\left(1 - \frac{Q^2_\mu(q)}{Q^2(q)}\right)\times \\ &\qquad\times\Big[A_V(p)A_V(k)K(p)\cdot K(k) + B_V(p)B_V(k)\Big] \\ &\quad - 2A_V(p)A_V(k)C_\mu(s)K_\mu(p)K_\mu(k) \\ &\quad + A_V(p)A_V(k)\frac{Q_\mu(q)}{Q^2(q)}\times \\ &\qquad\times\sum_\nu C_\nu(s)Q_\nu(q)\Big[K_\mu(p)K_\nu(k) + K_\mu(k)K_\nu(p)\Big] \\ &\quad + A_V(p)B_V(k)K_\mu(s)K_\mu(p) + A_V(k)B_V(p)K_\mu(s)K_\mu(k) \\ &\quad - \frac{K(s)\cdot Q(q)}{Q^2(q)}\Big[A_V(p)B_V(k)K_\mu(p) \\ &\qquad\qquad + A_V(k)B_V(p)K_\mu(k)\Big]Q_\mu(q) \\ &\quad - \frac{c_{\rm sw}}{2}C_\mu(\tfrac{q}{2})\Big\{A_V(p)B_V(k)\Big[K(p)\cdot K(q) - K_\mu(p)K_\mu(q)\Big] \\ &\qquad - A_V(k)B_V(p)\Big[K(k)\cdot K(q) - K_\mu(k)K_\mu(q)\Big]\Big\}\,.\end{aligned} \tag{14}$$

If we now choose to impose the condition $p_\mu = q_\mu = 0$, (14) simplifies to

$$\begin{aligned}\frac{1}{4}\,\mathrm{tr}\Big(\gamma_\mu\Gamma^{P(0)}_{I,\mu}(p,q)\Big) &= \frac{c_m}{D_I(p)D_I(k)}\times \\ &\times\Big\{A_V(p)A_V(k)K(p)\cdot K(k) + B_V(p)B_V(k) \\ &\quad - \frac{c_{\rm sw}}{2}\Big[A_V(p)B_V(k)K(p)\cdot K(q) \\ &\qquad - A_V(k)B_V(p)K(k)\cdot K(q)\Big]\Big\}\,.\end{aligned} \tag{15}$$

The tree-level correction is carried out by dividing the quantity obtained nonperturbatively from the lattice, corresponding to the lhs of (15), by the expression on the rhs of (15).

References

1. F.D.R. Bonnet et al., Phys. Rev. D64 (2001) 034501 [hep-lat/0101013].
2. P.O. Bowman et al., Phys. Rev. D70 (2004) 034509 [hep-lat/0402032].
3. A. Sternbeck et al., Phys. Rev. D72 (2005) 014507 [hep-lat/0506007].

4. C.S. Fischer and R. Alkofer, Phys. Rev. D67 (2003) 094020 [hep-ph/0301094].
5. A. Höll, A. Krassnigg and C.D. Roberts, Nucl. Phys. Proc. Suppl. 141 (2005) 47 [nucl-th/0408015].
6. H. Iida, M. Oka and H. Suganuma, Eur. Phys. J. A23 (2005) 305 [hep-ph/0312328].
7. C.S. Fischer, F. Llanes-Estrada and R. Alkofer, Nucl. Phys. Proc. Suppl. 141 (2005) 128 [hep-ph/0407294].
8. J.C.R. Bloch et al., Nucl. Phys. B687 (2004) 76 [hep-lat/0312036].
9. C.S. Fischer and R. Alkofer, Phys. Lett. B536 (2002) 177 [hep-ph/0202202].
10. R. Alkofer, C.S. Fischer and F.J. Llanes-Estrada, hep-ph/0607293.
11. J. Skullerud and A. Kızılersü, JHEP 09 (2002) 013 [hep-ph/0205318].
12. J.I. Skullerud et al., JHEP 04 (2003) 047 [hep-ph/0303176].
13. M.S. Bhagwat and P.C. Tandy, Phys. Rev. D70 (2004) 094039 [hep-ph/0407163].
14. J.I. Skullerud et al., Nucl. Phys. Proc. Suppl. 141 (2005) 244 [hep-lat/0408032].
15. UKQCD, K.C. Bowler et al., Phys. Rev. D62 (2000) 054506 [hep-lat/9910022].
16. W. Celmaster and R.J. Gonsalves, Phys. Rev. D20 (1979) 1420.
17. P.O. Bowman, U.M. Heller and A.G. Williams, Phys. Rev. D66 (2002) 014505 [hep-lat/0203001].